



## PERFORMANCE ANALYSIS FOR OPTIMIZED LIGHT WEIGHT CNN MODEL FOR LEUKEMIA DETECTION AND CLASSIFICATION USING MICROSCOPIC BLOOD SMEAR IMAGES

MAHMOUD SAED ALKHOULI\* AND HIREN JOSHI †

**Abstract.** The objective of this work is to create a diagnostic tool for the early diagnosis of leukaemia which is a serious type of cancer affecting bones and blood. Acute lymphoblastic leukemia (ALL) is the most dangerous form of leukemia. Doctors diagnose it by blood samples under powerful microscopes with enhanced lenses which can be slow and is sometimes affected by disagreements among experts. Therefore, the purpose of this work was to create a profound diagnostic tool for the early diagnosis of leukaemia. We propose an Optimized Light Weight CNN to detect ALL at the early stage. Fragmentation and classification based on preprocessing are the two main components of the suggested method. Artificial images are created during the segmentation process and then tamed by chromatic modification. The proposed model is used to extract the best deep features from every blood smear image to predict the presence of ALL. The work was tested by two lymphoblastic leukaemia image databases (ALL\_IDB1 and ALL\_IDB2). Deep-learning (DL) models-based segmentation and classification techniques have recently been introduced for detecting ALL; however they still have certain drawbacks. The proposed approach was assessed with few DL parameters like accuracy, F1 score, precision, recall and Area under the curve. In comparison to the most recent research studies already published; the suggested strategy produced exceptional classification accuracy as 99.56

**Key words:** Acute lymphoblastic leukaemia, Optimized Light Weight CNN, leukaemia, blood smear image.

**1. Introduction.** One of the most important elements of the human anatomy is blood. It contains RBCs (Red Blood Cells) and polypropylene or plasma [1]. Plasma makes up the majority of the blood's composition. White blood cells, commonly known as WBCs, platelets each make up less than one percent of the blood's total volume. Red Blood Cells, White blood cells and Platelets [2-4] are the three primary components of blood that may be distinguished by the blood's appearance, colour, size, chemical make-up, and texture, respectively. The RBC is the most significant type of blood sample, and one of its fundamental components is haemoglobin. Hemoglobin is responsible for the red colour of blood and is responsible for carrying oxygen to all regions of the body. When there is a fall in haemoglobin levels, there is also a decrease in oxygen, which causes exhaustion and weakness. There are four million to six million red blood cells in every individual micro liter of blood, which accounts for forty to forty-five percent of the total volume of blood [5]. WBCs protect us from pathogens and provide us antibodies and resilience; the number of WBCs that may be found in one micro liter of blood can range anywhere from 4000 to 10,000 [6]. Platelets have a concentration in the blood that ranges from 1 million to 5 million per micro liter and are responsible for the clotting process [7]. Therefore, alterations in the levels of any of the fundamental components of blood can result in adverse effects on a human's body, including conditions like neutropenia, leukaemia, and opathies. Because it encompasses both RBCs and platelets, a large WBC density is associated with a compromised immune system in the body. ALL), invasive lobular leukaemia, acute myeloblastic leukaemia, and chronic myeloblastic leukaemia are the four subtypes of leukaemia [8] that are recognized by professionals in the medical field. Chronic myeloblastic leukaemia is the most common form of the disease. Of them, acute lymphoblastic leukaemia (ALL) is the most prevalent, accounting for 70% of all instances of leukaemia, and the most deadly [9].

In addition, environmental factors as well as genetic predispositions play an important part in the progression of the disease. The excessive and inappropriate expansion of neutrophils in the bone marrow is the underlying cause of ALL [10]. ALL can be broken down into one of three different structural categories: S1, S2, S3 [9]. S1 cells are the tiniest and have the most homogenous population as well as abrasive chromatins.

---

\*Gujarat University, Ahmedabad, India ([al-khouli@hotmail.com](mailto:al-khouli@hotmail.com)).

†Gujarat University, Ahmedabad, India ([hdjoshi@gujaratuniversity.ac.in](mailto:hdjoshi@gujaratuniversity.ac.in)).

S2 cells are significantly bigger than S1 cells and have more nuclear variety than the S1 cells. S3 cells are larger than S1 cells and have compartments that protrude into the cell rather than being contained within the cell. Therefore, getting a timely diagnosis of ALL is extremely important for the healing process, especially for young children [10].

The fact that standard and lymphocytes cell types share numerous similarities, on the other hand, creates difficulties for early lymphocyte diagnosis [11]. As a consequence of this, lymphocytes were separated into three distinct categories: normal, unusual, and aggressive. Normal lymphocytes can be identified by their cohesiveness as well as their shaped, tiny, and jagged nuclei; unusual cells can be identified by their enormous diameter and nucleus as well as the fact that their chromatins are doughy; and aggressive cells can be identified by their homogeneity as well as the fact that they are surrounded by red cells. The different types of lymphocytes can be identified through a process called micron - sized investigation, which requires taking samples of bone marrow or blood and submitting them to a pathologist for analysis [12, 13].

However, a proper diagnosis of leukaemia requires the collection and analysis of a sample of bone marrow. As when the analysis is performed individually, it is arduous, time-consuming, and susceptible to divergent expert judgments. Therefore, the accuracy of a human diagnosis rests on the skill of the pathologist, despite the possibility of human mistake. Several studies have developed automated methods for identifying leukaemia by identifying WBC characteristics from micrographs. Thus, the automated classification of blood cell pictures will result in a speedy and accurate diagnosis and will make it possible to examine several cells from every individual. ML and DL can solve human diagnosis issues. It has been demonstrated that the convolutional neural network (CNN), which has an improved ability to discern between healthy and malignant cells, can assess and resolve many of the deficiencies of manual diagnostic and medical imaging.

In this investigation we used two publicly available dataset ALL-IDB1 and 2 to test support our proposed Optimized Light Weight CNN model. The work has also contributed in:

- Fragmentation and classification based on preprocessing are the two main components of the suggested method.
- Artificial images are created during the segmentation process and then tamed by chromatic modification. The proposed model is used to extract the best deep features from every blood smear image.
- A fine tuned technique was employed amongst CNN models to classify deep features and to achieve promising predictive performance.
- Blood microscopy image analysis systems were developed to aid bone marrow biopsies and professionals in making appropriate diagnostic judgments.

The article contains Literature review in Section 2. The methods and materials of the proposed work are explained in Section 3. Results are analyzed in Section 4 and the work is concluded in Section 6.

**2. Related work.** During the blood sample image optimization phase of the experiment conducted by authors of [14], the target region was improved, which had an effect on the segmentation outcome. The resampled and misleading edges of the photos created by Razzak et al [15] were eliminated utilizing wiener filter, which allowed the images to be improved. In order to produce high-quality segmented pictures, pre-processing techniques such as k-means, median filtering, and contrast stretching were performed by Manglem et al [16]. The images that were used in the research carried out by the authors were processed by making use of the HSV (hue, saturation, value), CMYK (cyan, magenta, yellow and key) and RGB (red, green, blue) colour spaces. HSV, in order to generate additional images for the purpose of identifying the characteristics that are most significant through the use of principal component analysis to acquire White blood cells nuclei which was proposed by Hellmich et al [17]. Authors Wang et al [18] initiated the DL strategy to leukocyte classifying and segmenting during or before and fragmentation steps. They then used a deep convolutional network to optimise the results, and then the DarkNet- and ShuffleNet models were used to extract deep features.

Authors of [19] improved images by reducing their luminance when transforming from RGB to HSV. They then used fcm method to separate the cores from the rest of the image (the hydrologic process breaks the relation between the clusters and the image context and then pulls out the largest significant design and analytical features), presented an intuitive method for improving images organized by ML algorithms. Scotti et al [20] Used DL techniques for cell radius convergence, image sharpening and shape etc.

Using segmentation with obscured C-means clustering and then classification with five different classifiers,

Satpatti et al [21] presented a statistical infinitesimal technique for discerning pernicious lymphocytes from normal capillary images and symptomatic lymphocytes. This method was accomplished by first using shadowed C-means clustering for segmentation. When evaluating leukaemia, Yaakob et al [22] described many phenotypic and ecological characteristics, and how these features were fed into four classification techniques; all of the algorithms obtained superior diagnosis outcomes across all age demographics. Alrefai et al [23] Performed feature selection that used the algorithm for particle swarm optimization using the ensemble learning approach, and then used five classification algorithms to score the features that were picked; the techniques produced favorable outcomes.

Mandal et al [24] Developed a technique for screening cancer cells that involves the extraction of critical traits (such as an enlarged nuclei and neighboring nuclei, both of which are indicative of cancer cells) through the utilization of various learning algorithms. Shah J.H et al [25] proposed an efficient method for analyzing the blood database for the purpose of treating leukocytes. This system consisted of the following phases: enhancing pictures, assembling wavelets, retraining the dataset, and categorizing the supplied classes through using CNN model.

Using DeepLabv3 and ResNet-50, Ameer et al [26] proposed a saliency detection method for extracting leukocytes from the remaining portion of the image in order to obtain deep feature maps; the system obtained good WBC recognition accuracy. Marr et al [27] performed an analysis using a CNN model as a component of training. They developed the model, and when the number of images increased while it was being trained, they came to the conclusion that the model was even more successful when it comes to the majority of training sets.

Pooja et al., [28] used T cells, or T lymphocytes, that are responsible for cell-mediated immunity. These cells mature in the thymus gland, from which they derive their name. There are various subtypes of T cells, each serving specific functions. Helper T cells (CD4+) assist other immune cells, activating both B cells and cytotoxic T cells. Jayachitra et al., [29] suggested Cytotoxic T cells (CD8+) in combating infections by attacking and destroying infected or damaged cells. On the other hand, Gupta et al.,[30] used B cells for conducting their investigation, where it contributes to immunity by generating antibodies that target specific pathogens.

**3. Methods and materials.** This part of the article contains the methods and materials used for the entire investigation Fig. 3.1 represents the proposed architecture.

**3.1. Dataset.** In this study, the publicly accessible ALL-IDB dataset, which contains specimens of blood samples, was used to test neural networks and other hybrids of DL models. The most deadly type of leukaemia, ALL, is the focus of the dataset. Experts in lymphoma have detected and categorized every lymphoma in each image. All of the photographs were captured with a fluorescence microscopy in a JPG format with a G5 PowerShot Canon camera with a high resolution of  $2592 \times 1944$ .

ALL-IDB datasets come in two varieties: ALL IDB1 (subset1) and ALL IDB2 (subset2). Around 108 total images, that has 49 lymphoma and 59 photographs of normal individuals, are included in the ALL-IDB1 collection. Each image shows over 39,000 blood components that have been categorized by lymphoma specialists. On the other hand, the ALL-IDB2 dataset has 260 and 130 of lymphomas and normal cells respectively. The blasted cells and healthy tissues from the ALL-IDB1 dataset were used to crop the ALLIDB2 dataset.

Samples from both datasets are shown in Fig. 3.2. The dataset is collected from <https://www.kaggle.com/nikhilsharma00/leukemia-dataset>.

**3.2. Image preprocessing.** The initial stage in imaging techniques is preprocessing. When examining blood samples underneath a microscope, the illumination of the microscope is altered to capture photographs of the samples. As a result, AI imaging approaches perform worse as a result of fluctuations in the luminance of the microscope and variations in reflections caused by light. So, using noise reduction algorithms can help you get better photographs. The photos in this study were improved by finding the parameters of the RGB colour streams, and the colors were then stabilized using cropping. The noise was then eliminated, and the contrast of the edges was improved using Laplacian filters until the image was smooth, the filter is gradually positioned around the image. Each central pixel was swapped out for an average of 35 nearby pixels to lessen the disparities between the pixels. Equ. 3.1 to Equ. 3.3 represents the average work of image preprocessing.  $y(m)$  represents the input,  $\omega^2 d$  represents the differential equation.

$$\text{Improvedimage} = y(m) - \mathcal{U}^2 d \quad (3.1)$$

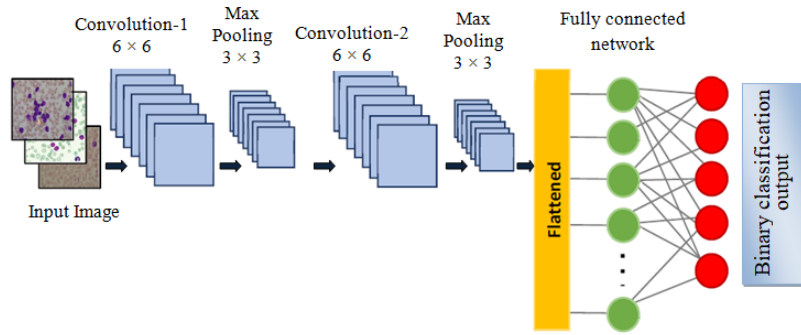


Fig. 3.1: Proposed architecture for Optimized Light Weight CNN

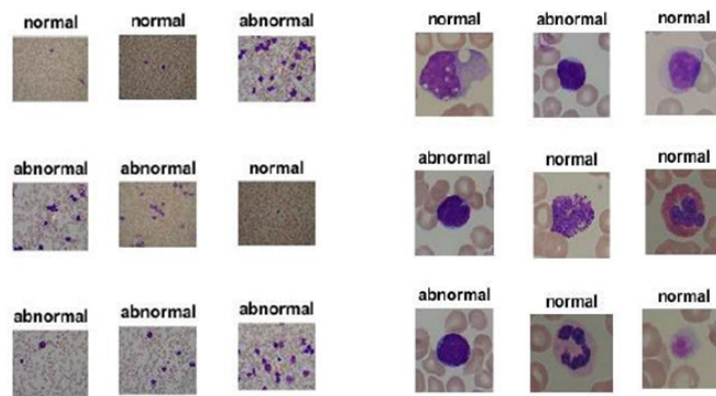


Fig. 3.2: Samples of Dataset (a) Subset1-ALL-IDB1 (b) Subset2-ALLIDB2

$$y(m) = m - 1 + \sum_{i=1}^m (y(m-1)) \quad (3.2)$$

$$U^2d = \frac{f(nx)}{(y)} + \frac{f(ny)}{(x)} \quad (3.3)$$

$y(m)$  is the input image,  $(m-1)$  represents the preceding input, and  $m$  represents the number of pixels present in the image. A Laplacian filter is used to reduce the noise in the image, which is represented in Equ. 3.3, in which  $x$  and  $y$  are the matrix coordinates. Finally an improved image is acquired by subtracting the value of the filtered image with the average  $y(m)$  obtained from Equ. 3.2. Few samples of the enhanced image is as shown in Fig. 3.3.

**3.3. Optimized Light Weight CNN.** Our proposed Optimized Light Weight CNN consists of Convolution, pooling, flattening layers, and multilevel hidden neurons made up the majority of the CNN architecture. Fully connected neural networks (FCNNs) used automatic extraction of characteristics from the input photos to classify them. Pooling layer and convolution layer were used to extract features. The features were obtained after binarizing the image in these layers, and the classification process was then initiated. Feature Learning, Receptive Fields, sharing information among parameters, structural arrangement, shift variance in pooling, non linear activations are the specific reasons for following a layered approach in the proposed method. The

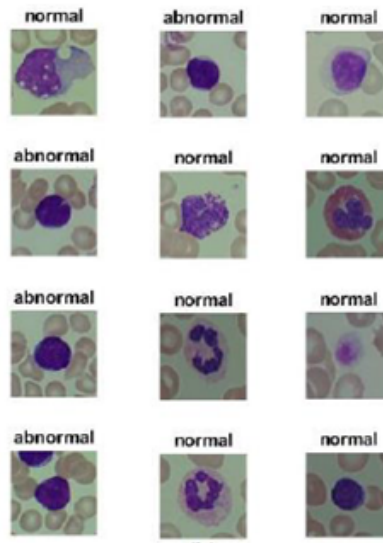


Fig. 3.3: Samples of improved image

specifics of the architecture we created are shown in Fig. 3.3. The phase wise explanation of the proposed model is explained as follows.

**Layer: 1-Convolution Layer** This layer is in charge of utilizing various attributes to investigate various filters on the source images. We utilized a CNN with a 64 feature map that was  $6 \times 6$  in size. The image was subjected to convolution filters through sliding. The settings for the filter were chosen at random. To prevent over fitting, we employed three convolutional layers.

**Layer: 2-Max Pooling Layer** The Max pooling layer is in charge of reducing the size of the segmented image to help it focus on any significant feature, region, or entity. We utilized a max-pooling layer in our network with a size of  $2 \times 2$ . We increased this layer's quantity by two.

**Layer: 3-Flattening Layer** A two-dimensional max-pooled matrix was converted into a one-dimensional array by this layer to ensure that each cell may serve as an input node for the entire connected network.

**Layer: 4-Fully connected Layer** With one input layer (in our example, the flattened layer), an output and hidden layer, this component was a naive linked complete forward network. The hidden layer in our model has 128 nodes, Dropout of 10 percent, and Batch-Normalization to reduce over fitting. The ReLU activation function had been applied for a straightforward computation. Two types of optimization techniques stochastic gradient descent and ADAM optimizers are set up at the output layer, each optimizer at a time. Each of the five output nodes we added, one for every leukaemia class and normal class samples which was managed by a Soft Max activation mechanism. Since this configuration was more appropriate for the sample size of dataset we employed, our Optimized Light Weight CNN model was trained with 30 epochs and 64 batch sizes. To get the optimal performance, different epoch counts were tested. Although we attempted to raise the number of epochs to 100, the additional running time was not significantly faster.

#### Algorithm 1: Optimized Lightweight CNN for Leukemia Detection

**Input:** Smear segmented images

**Output:** Leukemia classified images

Build the Optimized CNN model

##### 1. Convolutional Layers

```
model.add(layers.Conv2D(64,(6,6), activation='relu',
input_shape=(image_height, image_width, channels)))
model.add(layers.Conv2D(64, (6, 6), activation='relu'))
```

```
model.add (layers.Conv2D (64, (6, 6), activation='relu'))
```

## 2. Max Pooling Layers

```
model.add (layers.MaxPooling2D ((2, 2)))
```

```
model.add (layers.MaxPooling2D ((2, 2)))
```

## 3. Flattening Layer

```
model.add (layers.Flatten ())
```

## 4. Fully Connected Layer

```
model.add (layers.Dense (128, activation='relu'))
```

```
model.add (layers.Dropout (0.1))
```

```
model.add (layers.BatchNormalization ())
```

## 5. Output Layer

```
model.add (layers.Dense (num_classes, activation='softmax'))
```

```
return model
```

## 6. Model training and evaluation

```
train_model (model, train_data, validation_data, epochs, batch_size):
```

```
model.compile (optimizer='adam', loss='categorical_crossentropy',
```

```
metrics=['accuracy'])
```

```
model.fit (train_data, epochs=epochs, batch_size=batch_size,
```

```
validation_data=validation_data)
```

```
cnn_model = build_cnn_model ()
```

```
train_model (cnn_model, train_data, validation_data, epochs=30, batch_size=64)
```

**3.4. Experimental Analysis.** The convolutional layer is one of the most important layers. Equ. 3.4 describes how this layer conducts a linear operation known as convolution in between filter  $w(t)$  and the image  $x(t)$ . The convolution layer is governed by three variables: p.step, filter size and, zero padding. The enveloping around the images increases as the filter size increases. Every filter is intended to find particular elements throughout the input image. For instance, some filters are made to recognize edges, others to recognize geometric characteristics, and still others to recognize patterns and shades. Translation invariance is the term used to describe this characteristic of CNNs. To preserve the size of the original input, zero padding utilized. The convolutional filter and original input sizes are used to calculate the size of the zero pad. The number of steps the filter applies to the image at once is determined by the p-step parameter.

$$In(t) = (k*w)(r) = \int k(n)w(u-v) \cdot da \quad (3.4)$$

'In(t)' represents the input and 'u' and 'v' are the integer values. Using 'u' and 'v' the same two classes of normal and healthy, 'k(n)' represents the preceding input, 'w' as weights. We investigated developing a classification model in this experiment, where image transformation techniques were applied to ALL affected and not affected data. As a result, we used 275 samples for testing and 1000 samples for training for both classes. In addition, we used 5-fold cross validation in this study.

The dimensionality and color information of an image should be prioritised when implementing our Optimized Light Weight CNN model; as a result, convolutional filters are customised for the input images. Two-dimensional images are processed using the convolutional layer of the filter  $k_f$ , using image as the input, as illustrated in Equ. 3.5. The convolutional layers in the case of the RGB input images operate on separate two dimensional convolutions for every colour: R, G, and B. A rectified linear unit (ReLU) layer is added after a number of convolutional layers for additional processing. The negative input is inhibited and turned into 0 by this layer, which transmits the positive input. The ReLU layer only transmits positive characteristics and transforms negative values to zero, as shown in Equ. 3.6.

$$s(i, j) = (I * K)(i, j) = \sum_m \sum_n I(m, n)K(i-m, j-n) \quad (3.5)$$

$$ReLU(x) = \max(0, x) = \begin{cases} x, & x \geq 0 \\ 0, & x < 0 \end{cases} \quad (3.6)$$

Table 3.1: Data split for training and testing the proposed approach

Dataset	Phase	No. of samples
ALL_IDB1 (subset-1)	Training-80%	Leukemia Affected .....42 Leukemia Not Affected.....39
	Validation-10%	Leukemia Affected .....09 Leukemia Not Affected.....10
	Testing -10%	Leukemia Affected .....12 Leukemia Not Affected.....13
ALL_IDB2 (subset-1)	Training-80%	Leukemia Affected .....78 Leukemia Not Affected.....69
	Validation-10%	Leukemia Affected .....28 Leukemia Not Affected.....26
	Testing -10%	Leukemia Affected .....16 Leukemia Not Affected.....16

Before using any imagery transformation algorithms, we split the dataset in half, using 30 percent of the overall for testing and 70 percent for training. Then, in order to enhance the amount of data samples, we applied the image transformations to both portions. In each cross-validation iteration, we made sure that each dataset component had the same quantity of images with various folds. As a result, we ran our trials for each fold separately, after which we determined the accuracy and loss metrics for each fold. The final performance was expressed as a five-fold average. The data split for training and testing is shown in Table. 3.1.

Convolutional layers high amount of parameters, which leads to an over fitting issue. Our Optimized Light Weight CNN model offers a remedy for this issue by utilizing a dropout layer. Each time the dropout layer is used, 50 percent of the neurons are stopped and 50 percent are passed. The dropout layer in this investigation was adjusted at 50%. The training time is doubled by this layer. The training process is slowed down by the high-dimensional feature maps produced by convolutional layers. Thus, Our Optimized Light Weight CNN model offers a remedy for this issue by utilizing a dropout layer. Each time the dropout layer offer pooling layers to minimize the dimensionality in order to accelerate the training phase. The same convolutional layer technique powers interactions between pooling layers within CNNs.

$$P(i; j) = \max_{m,n=1\dots k} A[(i-1)p+m; (j-1)p+n] \quad (3.7)$$

$$P(i; j) = \frac{1}{k^2} \sum_{m,n=1\dots k} A[(i-1)p+m; (j-1)p+n] \quad (3.8)$$

The max and average-pooling layers are two different categories of pooling layers. Equ. 3.7 illustrates how the upper limit is selected when employing the max-pooling layer work. On the other hand, the average specified values are calculated and replaced by the average value in the average-pooling layer work mechanism, as indicated in Equ. 3.8.

In our Optimized Light Weight CNN the layer in charge of classification is the FCL. All neurons are connected to one another within the FCL. Two dimensional feature maps are transformed into one-dimensional maps using the FCL layer. Different CNNs have different numbers of FCLs; some networks have more than one FCL, which assigns each image to the appropriate class. Finally, the softmax activation function receives the FCL result and generates neurons with the same amount of classes supplied. Softmax developed two types of neurons for this study: leukaemia affected and normal.

The proposed investigation was conducted as follows: TensorFlow and OpenCV were utilized for image preprocessing. Python was used for this deep learning scripting. Development of the model was facilitated by employing an Integrated Development Environment (IDE) Jupyter Notebooks and effective collaboration was maintained through version control using Git. Model evaluation tools, including metrics such as accuracy and F1-score, were integrated, along with data annotation tool Labelbox for preparing datasets. A GPU,

Table 4.1: Results obtained from the proposed approach

Model Classification	Training Accuracy	Validation Accuracy	Training Loss	Validation Loss
Leukaemia Affected	99.46 %	94.93 %	0.00362	1.2462
Leukaemia not Affected	99.67 %	92.45 %	0.00594	0.8357
<b>Average Assessment</b>	<b>99.56 %</b>	<b>93.68 %</b>	<b>0.00478</b>	<b>1.04095</b>

from the NVIDIA GeForce RTX series was used to expedite the computationally intensive training process, while general computation and data handling were necessitated by a multi-core CPU, 16GB RAM. Docker for containerization and optimization libraries Intel's MKL are also used. The model was experimented in 80:20 ratio where 80 per cent of the input images are used for testing and remaining 20 per cent for testing the model.

**3.5. Model Evaluation.** We chose 2 key criteria for measuring the performance of our proposed Optimized Light Weight CNN in order to evaluate our model. The first measure of accuracy was the proportion of consistently categorized input images among all samples. We evaluated our model by 1. Training accuracy, which assesses how well the model performs during training, and validation accuracy, which demonstrates how well the model performs while classifying unknown data. 2. The loss metric concentrates on figuring out the prediction error and is utilized to modify the weights of nodes. Additionally, the training loss and validation loss is also computed.

**4. Results and Discussion.** The overall summary of the findings of our investigation trial which is assessed with few DL parameters like accuracy, F1 score, recall, precision and AUC that are as represented in Table 4.1. Using the input samples, we were able to classify leukaemia affected and not affected in binary form with the best performance which records the recognition accuracy as 99.56%. The model identified more complexity to distinguish between the classes as there are more classes adhered to and included in a classification process. In terms of accuracy and loss measures, we found that SGD optimizer performs significantly better than ADAM optimizer.

Additionally, we found that extended epoch iterations had little effect on the model's performance. One of the benefits of our proposed approach is that they are resource-flexible because they just need computers with moderate requirements, as opposed to other existing models, which need machines with high specifications. In addition, our proposed approach differs from CNN models in that they train more quickly. CNN models require a lot of training time whereas our approach utilized less amount of time for classification and recognition. The time concern of the proposed method is noted by the Receiver operating curve values obtained which is discussed in further part of this section.

The results of each fold's performance for our proposed approach are shown in Table 4.2. In binary classification, fold 4 received the highest score. We can draw the conclusion that the performance results may vary greatly depending on the samples used for the test and training set. We assessed our strategy using 5-fold cross-validation since several fold cross validation continues to produce more trustworthy outcomes in evaluation. Table 4.3 provides the final overall performance metrics assessed with respect to ML parameters

The proposed Optimized Light Weight CNN for the early detection of leukaemia using two named datasets is depicted in Fig. 4.1 by the confusion matrix. All dataset samples that were wrongly identified in the auxiliary diameter (True\_Positive and True\_Negative) but correctly labelled in the prime diameter (True\_positive and True\_negatives) are included in the confusion matrix (False\_Positive and False\_Negative).

Cross-entropy, a measurement of the error rate between the observed and projected outputs, is one way to assess how well the deep learning models. Fig. 4.2 displays the training, testing and validation results of our approach. The performance is shown in three different colors: red when testing, blue for training, and green throughout validation. The intersecting lines were used to obtain the optimum performance. As the number of epochs progressed, the error rate between the actual and expected outputs reduced; the training ended when

Table 4.2: Folds wise results of the proposed approach

Model Classification	Training Accuracy	Validation Accuracy	Training Loss	Validation Loss
Fold-1	99.46%	94.93%	0.00362	1.2462
Fold-2	99.82%	93.98%	0.10478	0.0098
Fold-3	99.29%	93.79%	0.00982	1.1062
Fold-4	99.73%	94.68%	0.00327	0.9834
Fold-5	99.58%	94.82%	1.00387	0.7263
<b>Average</b>	<b>99.56%</b>	<b>93.68%</b>	<b>0.003997</b>	<b>0.9978</b>

Table 4.3: Overall results of the proposed approach

Model Classification	Accuracy	Precision	Recall	Sensitivity	F1 Score	Error rate
Leukaemia Affected	99.46 %	98.91 %	97.11 %	98.62 %	99.15 %	0.0026
Leukaemia not Affected	99.67 %	99.43 %	99.38 %	98.79 %	98.93 %	0.1935

Predicted Class	116 58.2%	0 0.0%	0.0% 100%
	0 0.0%	121 41.8%	0.0% 100%
	0.0% 100%	0.0% 100%	0.0% 100%
Target Class			

Fig. 4.1: Confusion Matrix

the method's least error value was reached. The proposed model's best validation result was 0.034817 during the fifth epoch, and other phases showed the same performance.

The execution time of our approach is recorded and assessed in terms of Receiver Operating Curve (ROC). This curve exhibits the graphical performance of the model. Fig. 4.3 depicts the ROC of our proposed approach.

The performance of our suggested pertinent systems is compared to the evaluation findings of earlier systems in Table 4.4. The accuracy of the prior systems ranged from 89% to maximum of 93% that of our proposed system was 99.5%. The existing systems' precision levels were 90% and 94% respectively, but our suggested system was 98%.

The sensitivity of the compared existing systems ranged from 89% to 93%, but the recall of the system we proposed was 99.38%. In terms of specificity, the earlier methods achieved 89% and 94%, but our suggested solution achieved 99.03%. The prior systems' AUCs were 83% and 97%, whereas our approach attained 99.21%.

**5. Conclusion.** In the medical field, AI technologies have surfaced to offer analytical ability and diagnosing tools with maximum reliability. Techniques utilizing ML and DL algorithms solve issues with conventional diagnosis limitations, expert disagreements, time-consuming monitoring of blood samples. These methods are

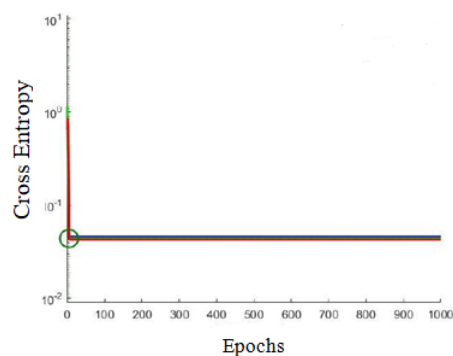


Fig. 4.2: Performance measure of the proposed approach

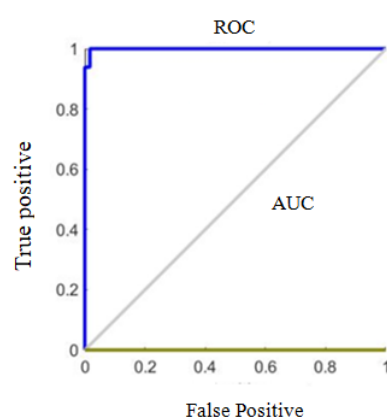


Fig. 4.3: ROC and AUC values obtained for the proposed model

Table 4.4: Existing versus proposed approach

Model	Accuracy (%)	F1 Score (%)	Specificity (%)	Recall (%)	Precision (%)	Error rate	AUC (%)
Inception V3	89.32	90.32	89.60	93.44	90.61	0.426	97.43
DCNN	92.43	89.85	93.21	89.42	91.92	0.392	83.82
AlexNet	93.15	91.37	94.84	89.28	94.76	0.562	92.46
Proposed approach	<b>99.56</b>	<b>99.53</b>	<b>98.79</b>	<b>99.38</b>	<b>98.91</b>	<b>0.01</b>	<b>99.21</b>

essential for the early identification of leukaemia. It affects white blood cells, bone marrow, and the immune system. Blood smears are the frequent diagnostic tool. In this paper, we described a new method for diagnosing leukaemia from microscopic blood pictures utilizing an Optimized Light Weight CNN. Our model established its ability by employing data augmentation strategies to overcome the over fitting problem. It surpassed previous machine learning methods by reaching 99.56% accuracy for binary classification of one leukaemia type as affected and not affected. All experiments included cross-validation. Medical picture categorization takes a long time to execute, but it's crucial to make sure the model is stable throughout. In the upcoming phases, there are plans to broaden this research by delving into quantum computing algorithms to enhance the precision of White Blood Cell (WBC) detection. Subsequent efforts will include the implementation of a hybrid approach,

integrating features derived from pre trained CNN models with those obtained from Spatial Pattern Analysis, Gray Tone Spatial Relationships, and Self-Similarity Encoding algorithms in a comprehensive feature vector. This combined feature vector will then be fed to Feed forward Neural Networks, for image classification.

## REFERENCES

- [1] Huang, N.T et al, "A micro fluidic device for simultaneous extraction of plasma, red blood cells, and on-chip white blood cell trapping". *Scientific Report*, 2018, 8, 1–9.
- [2] Dhiman, G., Vinoth Kumar, V., Kaur, A., and Sharma, A. "Don: deep learning and optimization-based framework for detection of novel coronavirus disease using x-ray images." *Interdisciplinary Sciences: Computational Life Sciences*, 2021, 13, 260-272.
- [3] Zadeh, H et al. "Automatic recognition of five types of white blood cells in peripheral blood". *Computerized Medical Imaging and Graphics* 2011, 35, 333–343
- [4] Nabavi, S.M.and Nabavi et al, "Flavonoids and platelet aggregation: A brief review." *European Journal of Pharmacology*, 2017, 807, 91–101
- [5] Al-Megren and S. Kurdi et al, "Red blood cell segmentation by thresholding and canny detector". *Procedia Computer Science*, 2018, 141, 327–334.
- [6] Natarajan, R., Lokesh, G. H., Flammini, F., Premkumar, A., Venkatesan, V. K., and Gupta, S. K. "A Novel Framework on Security and Energy Enhancement Based on Internet of Medical Things for Healthcare 5.0." *Infrastructures*, 2023, 8(2), 22.
- [7] Heemskerk P.E and, J.Wen et al. "Platelet biology and functions: New concepts and clinical perspectives". *Nature Reviews Cardiology*, 2019, 16, 166–179.
- [8] Sawyers and Denny, "Leukemia and the disruption of normal hematopoiesis." *Cell* 1991, 64, 337–350.
- [9] Messmore and H.L, "Wintrob's Atlas of Clinical Hematology." *JAMA* 2007, 297, 2641–2645.
- [10] S. T. Ahmed, V. V. Kumar and J. Kim, "AITel: eHealth Augmented-Intelligence-Based Telemedicine Resource Recommendation Framework for IoT Devices in Smart Cities," in *IEEE Internet of Things Journal*, 2023, vol. 10, no. 21, pp. 18461-18468.
- [11] Fati S.M et al." Score and Correlation Coefficient-Based Feature Selection for Predicting Heart Failure Diagnosis by Using Machine Learning Algorithms". *Computational and Mathematical Methods in Medicine*, 2021, 85003.
- [12] Nam, Y. and Raza, M. "3D semantic deep learning networks for leukemia detection." *Computers, Materials & Continua* 2021, 69, 785–799.
- [13] Muthukumar, V., Joseph, R. B., and Uday, A. K. "Intelligent medical data analytics using classifiers and clusters in machine learning." In *Handbook of Research on Innovations and Applications of AI, IoT, and Cognitive Technologies*, 2021, pp. 321-335.
- [14] Ramaneswaran, and Srinivasan, K et al "Hybrid Inception v3 XG Boost Model for Acute Lymphoblastic Leukemia Classification." *Computational and Mathematical Methods in Medicine* 2021, 2021, 2577375.
- [15] Razzak et al, "M.I. Efficient leukocyte segmentation and recognition in peripheral blood image Technology," *Health Care* 2016, 24, 335–347.
- [16] Dhanachandra, N and Manglem, K. "Image Segmentation Using K -means Clustering Algorithm and Subtractive Clustering Algorithm". *Proceedings Computer Science*. 2015, 54, 764–777.
- [17] Hellmich, H.L et al. "Principal component analysis of blood micro RNA datasets facilitates diagnosis of diverse diseases." *PLoS ONE*, 2020, 15, e0234185.
- [18] Iqbal, M and Wang, S.H.et al "A deep network designed for segmentation and classification of leukemia using fusion of the transfer learning models." *Complex and Intelligent Systems* 2021, 1, 1–16.
- [19] Mirmohammadi, P et al, "A Recognition of acute lymphoblastic leukemia and lymphocytes cell Subtypes in microscopic images using random forest classifier". *Physical and Engineering Sciences in Medicine*, 2021, 44, 433–444.
- [20] Scotti, F et al. "ALL Detection Based on Adaptive Unsharpening and DL". In *Proceedings of the ICASSP 2021-2021 IEEE Internl. Conf. on Acoustics Speech and Signal Processing* Toronto, ON, Canada, 6–11 June 2021, pp. 1205–1209.
- [21] Satpathy, S et al. "An ensemble classifier system for early diagnosis of acute lymphoblastic leukemia in blood microscopic images". *Neural Computing and applications*, 2014, 24, 1887–1904
- [22] Yaqoob, M. et al., "Identification of significant risks in pediatric acute lymphoblastic leukemia through machine learning (ML) approach." *Medical & Biological Engineering & Computing*, 2020, 58, 2631–2640
- [23] Alrefai, N. "Ensemble ML for Leukemia Cancer Diagnosis based on Microarray Datasets." *International Journal of Applied Engineering Research*, 2019, 14, 4077–4084.
- [24] Rajagopalan, V and Mandal et al. "ML based system for automatic detection of leukemia cancer cell". In *Proc. of the 2019 IEEE 16th India Council Internl. Conf. (INDICON)*, Rajkot, India, 13–15 December 2019; pp. 1–4.
- [25] Shah, J.H. and Fernandes, S.L." Robust discrimination of leukocytes protuberant types for early diagnosis of leukemia". *Journal of Mechanics in Medicine and Biology* 2019, 19, 1950055.
- [26] Ameer, P.M et al. "Segmentation of leukocyte by semantic segmentation model: A DL approach". *Biomedical Signal Processing and Control*, 2021, 65, 102385.
- [27] Bosna.D.and Marr, C et al." Tens of images can suffice to train neural networks for malignant leukocyte detection." *Scientific Reports* 2021, 11, 1–8.
- [28] Pooja, S. and Megha, G.S. "Using CNN to Detect Cancerous Cells in White Blood Cells from Bone Marrow through

- Microscopic Images.*" Journal of Advancement in Parallel Computing, 2021, 4(2).
- [29] Jayachitra, J. and Umakathaf, N. March. "Blood Cancer Identification using Hybrid Ensemble Deep Learning Technique." *In 2023 Second International Conference on Electronics and Renewable Systems (ICEARS) , 2023, pp. 1194-1198. IEEE.*
- [30] Gupta, R., Gehlot, S. and Gupta, A. "C-NMC: B-lineage acute lymphoblastic leukaemia: A blood cancer dataset." *Medical Engineering and Physics*, 2022, 103, p.103793.
- [31] Available: <https://www.kaggle.com/nikhilsharma00/leukemia-dataset>.

*Edited by:* Polinpapilinho Katina

*Special issue on:* Scalable Dew Computing for Future Generation IoT Systems

*Received:* Nov 4, 2023

*Accepted:* Jan 8, 2024